Vol. 20, No. 2 (2021) 885-897
Revista Mexicana de Ingeniería Química

Image segmentation with fast distance transform (FDT) and morphological skeleton in microalgae Raceway culture systems applications

Segmentación de imágenes con la transformada de distancia rápida y esqueleto morfológico en aplicaciones de sistemas de cultivo de microalgas Raceway

S.-S. Bautista-Monroy[1], J.-C. Salgado-Ramírez[2], C-A. Gómez-Aldapa[3], A. Téllez-Jurado[1], R. Ortega-Palacios[2], J. C. Jiménez-Escalona[4], A. Cadena-Ramírez[1]*

[1]*Posgrado en Biotecnología.* [2]*Programa de Ingeniería Biomédica; Universidad Politécnica de Pachuca, Carretera Pachuca-Cd. Sahagún, km 20, Ex-Hacienda de Santa Bárbara, C.P. 43830, Zempoala, Hidalgo, México.*
[3]*Área Académica de Química, Instituto de Ciencias Básicas e Ingeniería, UAEH, Ciudad del Conocimiento, Carretera Pachuca-Tulancingo, km 4.5, Col. Carboneras, C.P 42184, Mineral de la Reforma, Hidalgo, México.*
[4]*Instituto Politécnico Nacional, ESIME-TICOMAN, Section of postgraduate studies, México City, C.P 07340 Méx*

Received: December, 2020; Accepted: March 6, 2021

Abstract

Image segmentation is an important process in digital image analysis, there are several algorithms to carry out this process. In this work, an algorithm little studied in the segmentation of images is defined and that is also applicable in the processing of videos of biological systems, especially, the cultivation of microalgae in Raceway bioreactors. This algorithm is known as the Fast Distance Transform (FDT) and when operating it with the morphological skeleton, an algorithm capable of determining the number of objects in an image. Performs a separation when there is agglomeration due to the quantity and proximity of the objects and rebuild them regardless of the geometric shape they present, through the maximum points of brightness, centroids and area. With the above, it is possible to give individual monitoring, to describe the behavior of microalgae inside a Raceway bioreactor.

Keywords: Fast Distance Transform (FDT), morphological skeleton, image segmentation, bioreactor, videos.

Resumen

La segmentación de imágenes es un proceso importante en el análisis digital de imágenes, existen varios algoritmos para llevar a cabo este proceso. En este trabajo, se define un algoritmo poco estudiado en la segmentación de imágenes y que además, es aplicable en el procesamiento de videos de sistemas biológicos, en especial, el cultivo de microalgas en biorreactores Raceway. Este algoritmo se conoce como la Transformada Rápida de Distancia (TRD) y al operarla con el esqueleto morfológico se genera un algoritmo capaz de determinar el número de objetos en una imagen. Realiza una separación cuando existe aglomeración debido a la cantidad y proximidad de objetos y reconstruye sin importar la forma geométrica que presenten, a través de los puntos máximos de brillo, centroides y área. Logrando dar seguimiento individual, para describir el comportamiento de microalgas dentro de un biorreactor Raceway.

Palabras clave: Transformada Rápida de Distancia (TRD), esqueleto morfológico, segmentación de imágenes, biorreactor, videos.

1 Introduction

Artificial vision or computer-assisted vision simulates human visual processes and has various applications, such as: obtaining the distance of objects in the scene, detection of moving objects, recognition of patterns and shapes, among others. It is based mainly on obtaining frames, using light-sensitive digital cameras, any type of camera can be used (Loaiza *et al*., 2012; Amaya-Zapata *et al*., 2016; Borji, 2018). However, in these analyzes, image quality is of utmost importance, so the use of high-resolution cameras is recommended. In digital processing (artificial vision), two fundamental actions are sought: the improvement of the image to eliminate non-useful information and the extraction of information for automatic decision-

* *Corresponding author. E-mail*: arturocadena@upp.edu.mx
https://doi.org/10.24275/rmiq/Cat2294
ISSN:1665-2738, *issn-e*: 2395-8472

making (La Serna and Román, 2009).

Within the processing, several techniques are used, one of them is segmentation, that is, the process of regionalizing an image for a better analysis of the information (Loaiza *et al*., 2012).

In this sense, segmentation plays an important role in processing and is considered the first step in object recognition (Hanbury and Marcotegui, 2008). It consists of dividing an image into homogeneous regions, to separate the parts of interest. Edges, lines or curves can be identified, depending on the problem to be solved (La Serna and Román, 2009; Yu *et al*., 2017). In addition, segmentation is one of the main problems in image analysis, which is why several methods have been developed to perform the procedure (Akhlaghian *et al*., 2005; Liu *et al*., 2018).

An example of these methods is the distance map, through which a two-dimensional image can be projected. First, the distance transform (DT) is applied to a binary image, another is obtained in shades of gray and each value represents the numerical distance that each point (pixel) has with respect to its complement (Sotaquirá *et al*., 2005; Arcelli *et al*., 2009; Hernandez-Aguirre *et al*., 2019). DT has a computational complexity $O(N^2)$ while the Fast Distance Transform (FDT) is computationally complex O(N) ergo. The FDT is faster, hence its name (Salgado, 2011), for this reason it was chosen to monitor tracer particles that describe the hydrodynamic behavior in Raceway bioreactors, which are open systems for the cultivation of microalgae (Rodríguez-Mata *et al*., 2019; Solis-Méndez *et al*., 2020). The FDT transform a binary image to an image in shades of gray, where each shade of gray represents an integer numerical value which it will call the distance value of a white pixel with respect to its complement (black pixels) see Figure 1 A and B. The FDT per se does not allow segmenting, so other processes are necessary. It is here where the morphological skeleton plays an important role to perform image segmentation based on the FDT, see Figure 1 C.

The FDT has not been exploited in the hydrodynamic study of bioreactors, due to commercial particle image velocimetry systems are used (PIV) by cross-correlation algorithm to describe the displacement of the tracer (Zeng *et al*., 2016). In addition, image analysis through segmentation and distance maps has been focused on other areas such as the coffee study by Fourier transform (Hernandez-Aguirre *et al*., 2019). On the other hand, any information contained in a digital image, regardless of the area to which it belongs, can be extracted using the appropriate processing technique.

A color or gray scale frame has many fields of application such as: medical, military, biological, industrial, even in food analysis (Bai *et al*., 2014; Zhang *et al*., 2015; Hernandez-Aguirre *et al*., 2019). In previous studies (Bautista-Monroy *et al*., 2019) a low-density particle tracking and image processing method applied to Raceway bioreactors was developed. In this work, it was found that the flow patterns, the velocity of the liquid medium and the percentage of dead zones vary depending on the geometry of the agitator and the angular velocity. In the following work, an improvement of the particle tracking method proposed by (Bautista-Monroy *et al*., 2019) is proposed, using a greater number of tracer particles. In order to describe the hydrodynamic behavior in bioreactors, various techniques have been developed. Some of them involve the use of radioactive particles, spheres of some materials that simulate conditions of a certain substance and computational simulations that involve the growth of microalgae (Sabri, *et al*., 2018; Lizardi-Jiménez and Gutiérrez-Rojas, 2011; Rarrek, *et al*., 2019).

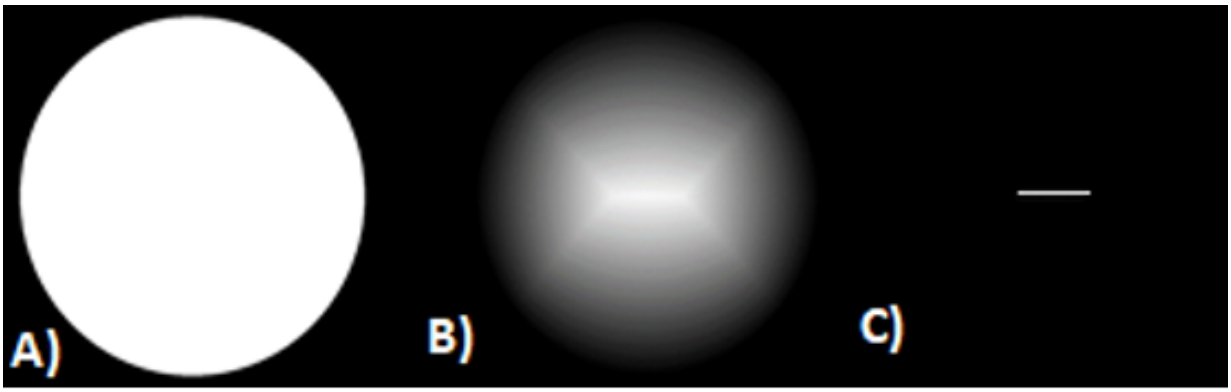

Fig. 1. A) binary image. B) result of FDT. C) morphological skeleton obtained from the FDT.

This research focuses on the binary image processing of a Raceway bioreactor, which is widely used for the cultivation of microalgae (Kanhaiya *et al*., 2015: May-Cua *et al*., 2019). The bioreactor contains tracer particles that simulate the density and particle size of some microalgae. This type of microspheres, like biomass, agglomerate due to the large amount contained and the flow currents that are generated within the system. It is extremely important to individually monitor each one of the particles, to simulate the behavior of these microorganisms within the Raceway. This is why image processing and the application of FDT are implemented to study the behavior of tracers, which is reflected in collisions between them and flow patterns. This document is organized as follows: Section 2 describes the methodology used, starting with the formal definition of FDT, mathematical morphology definitions and the definition of the morphological skeleton algorithm. As well as the systems conditions and the algorithms described application, that lead to the segmentation model proposed in this work. Section 3, the results are presented in conjunction with the discussion of them. And in section 4, a brief conclusion of the work is included.

2 Materials and methods

2.1 FDT

To describe the algorithms used, it is necessary to state some definitions.

Definition 1. Metric spaces. Let X be a set. A metric on X, called distance in a function $d : X \times X \rightarrow \mathbb{R}^+ \bigcup\{0\}$, such that:

$$\begin{aligned} d(x,y) = 0 &\longleftrightarrow x = y \quad \text{with} \quad x,y \in X \\ d(x,y) &= d(y,x) \quad \forall x,y \in X \\ d(x,y) &\leq d(x,z) + d(z,y), \quad \forall x,y,z \in X \end{aligned}$$

So the pair (X,d) is called the metric space. If d is a metric, $X = \mathbb{Z}$ and $d : X \times X \rightarrow \mathbb{Z}^+ \bigcup\{0\}$ then d is a discrete metric.

Definition 2. Metrics. Let $p = (x,y)$, $q = (u,v)$ points on $\mathbb{Z}^2$

$$\begin{aligned} &1.\ d_4(p,q) = |x-u| + |y-v| \\ &2.\ d_8(p,q) = \max\{|x-u|, |y-u|\} \end{aligned}$$

These metrics are called closed discs of radius 1, which correspond to the $k-neighborhoods$, where $k \in \{4,8\}$ and the distances are expressed as d_k. These $k-neighborhoods$ are widely used in digital image processing.

Definition 3. Distance Transform. Mapping DT:

$$\begin{aligned} R \subset X \subseteq &\mathbb{Z}^2 \\ f : X \rightarrow &\{0,1\} \\ f(x) = 1 \longleftrightarrow x \in R \quad y \quad f(x) = 0 &\longleftrightarrow x \notin \mathbb{R} \\ F = &\{(x, f(x)) | x \in X\} \\ \delta : X \rightarrow &\mathbb{Z}^+ \\ \delta(x) = \min&\{d(x,y) | y \in X - R\} \\ \Delta = &\{(x, \delta(x)) | x \in X\} \\ TD : F \rightarrow &\Delta \\ TD((x,f(x)) = &(x,\delta(x)) \end{aligned}$$

where $d \in \{d_4, d_8\}$,F is a **binary image**, Δ is called the **Distance transform**, the function δ is the **distance transformation** and R is the interest region.

The following distances are the most common functions for obtaining distance measurements:

1. *Euclidean*. $d([\mathbf{x},\mathbf{y}],[\mathbf{i},\mathbf{j}]) = \sqrt{(\mathbf{x}-\mathbf{i})^2 + (\mathbf{y}-\mathbf{j})^2}$
2. *City − Block*. $d([\mathbf{x},\mathbf{y}],[\mathbf{i},\mathbf{j}]) = |\mathbf{x}-\mathbf{i}| + |\mathbf{y}-\mathbf{j}|$
3. *Chessboard*. $d([\mathbf{x},\mathbf{y}],[\mathbf{i},\mathbf{j}]) = \max(|\mathbf{x}-\mathbf{i}|, |\mathbf{y}-\mathbf{j}|)$

Definition 4. FDT (Salgado, 2011). If d is one of the metrics d_4 o d_8 and $N(c) = \{p_i \in \mathbb{Z}^2 | d(c,p_i) = 1\}$, for $c, p_i \in \mathbb{Z}^2$ y $c \neq p_i$ we have:

$$\begin{aligned} &1.\ d(c,p) = \min\{d(p,p_i) : p_i \in N(c)\} + 1 \\ &2.\ d(c,p) = \max\{d(p,p_i) : p_i \in N(c)\} - 1 \end{aligned}$$

Through the distance transform of the neighbors of c we can find the distance transformation $\delta(c)$, where $\delta(c) = \min\{\delta(c) + 1\}$. With this it is established that the fast distance transform is obtained in 2 steps:

Sweep the binary image from top to bottom and from left to right. For each pixel $c \in R$, where R is the interest region, we assign $\delta(c) = 1 + \min(\delta(p_j) : p_j \in E)$ where E is one of the following sets shown in Figure 2.

Sweep the binary image from bottom to top and from right to left. For each pixel $c \in R$, where R is the interest region, we assign: $\delta(c) = \min\{\delta(c), 1 + \min\{\delta(p_i) : p_i \in D\}\}$, where D is one of the following sets shown in Figure 3.

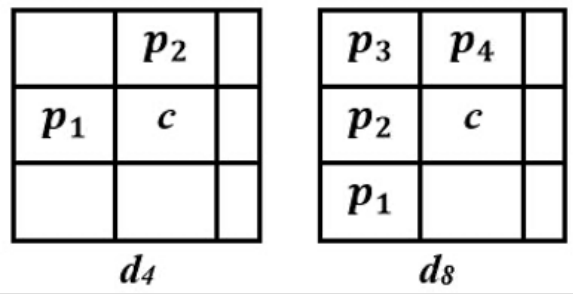

Fig. 2. Metric set for E.

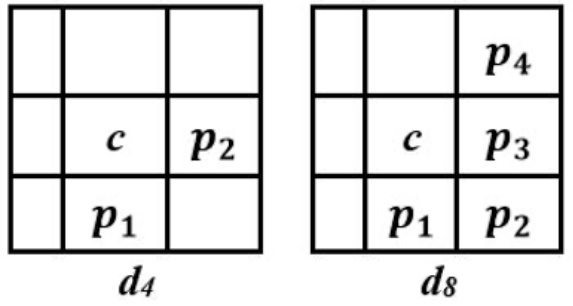

Fig. 3. Metric set for D.

The FDT algorithm is shown in the appendix A.

Mathematical Morphology and Morphological Skeleton

Mathematical morphology is based on 4 basic operations, these are defined as:

Definition 5. Erosion. $A \ominus B = \bigcap_{b \in B}(A)_b$

Definition 6. Dilation. $A \oplus B = \bigcap_{(} b \in B)(A)_b$

Definition 7. Opening. $A \circ B = (A \ominus B) \oplus B$

Definition 8. Locking. $A \odot B = (A \oplus B) \ominus B$

where A represents a binary image and B is a $k-$*neighborhood*. The erosion and dilation operations are a sweep of the image from left to right and from top to bottom where, when finding a pixel of interest in the binary image, a convolution is performed as shown in Definitions 5 and 6 in the region delimited by the $k-$*neighborhoods*.

Definition 9. Morphological skeleton. $\delta = \max(\delta(p_j) : p_j \in H)$ where H is a d_k metric as shown in Definition 2.

Definition 9 specifies the operation of the morphological skeleton algorithm on the FDT, that is, on δ. The algorithm consists of sweeping from left to right and from top to bottom. Finding a distance $\delta(p_i)$ determines the maximum value of distance delimited by the region of H and this value is assigned white and all other distances delimited by H are assigned the color black. The algorithm is as follows:

```
1  for y = 1 to δ→ High−1
3       for y = 0 to δ→ Width−1
4            a = δ→getPixel (x, y)
5            if a
6                 for k=y−1 to k<y+2
7                    for j=x−1 to j<x+2
8                       if δ→putPixel (x, y) < δ→putPixel (k, j)
9                          λ→putPixel (x, y) = white;
10                   else
11                      λ→putPixel (x, y) = black;
11                end
12             end
13          end
14    end
15 end
```

Centroids calculation

Definition 10. Centroid $X_c = \frac{1}{A}\sum_{i=1}^{N} x$ and Centroid $Y_c = \frac{1}{A}\sum_{i=1}^{M} y$, where A is the area of the geometric figure in the image. N are the columns, M are the rows and x and y represents the (x,y) coordinate of the image.

Definition 10 establishes a sweep, from left to right, from top to bottom in a binary image. If (x,y) coordinate is a white pixel will be counted x and y.

Definition 11. Binarized.

$$g(x,y) = \begin{cases} 1 & \text{if} \quad f(x,y) > threshold \\ 0 & EOC \end{cases}$$

Definition 11 details the binarization of an image based on a threshold. The algorithm consists of sweeping the image in shades of gray from left to right and from top to bottom. The pixel in the coordinate (x,y) located the sweep will be compared with the value of the threshold defined, if the value is greater than the threshold, the color white is assigned in (x,y), otherwise (EOC) is assigned the color black.

Tracer particles

To simulate the microalgae particles, 20 microcapsules of Sodium Alginate and Uranine (sodium fluorescein) were used. The particles were obtained in the following way: 10 g of Uranine and 6 g of Sodium Alginate were diluted in 200 mL of distilled water. This solution was passed through a capillary focusing chamber from which drops were dropped into a maturing solution (HCl and NaOH with pH between 5-8) and allowed to stand for 20 minutes, in order to maintain the intense coloration and bright of the Uranina. These particles have a diameter of 100 μm and a density of 654 Kg/m^3, which is similar to the cell density of some microalgae, such as *Arthrospira maxima*. These conditions ensure that the microspheres are carried away by the flow currents generated within the Raceway bioreactor (Bautista-Monroy *et al*., 2019).

Establishment of the bioreactor and system conditions

The Raceway bioreactor used has the following dimensions: 70 cm in length, 20 cm in total width, 10 cm in channel width and 8 cm in depth (Bautista-Monroy *et al*., 2019). It is provided with a 6-blade curved turbine-type mechanical agitator, driven by a Nema 17 bipolar stepper motor, with an angular speed of 35 rpm. A digital camera was placed 53.5 cm high (Sunco 12 megapixel resolution). The system was kept in a dark room, illuminated with an ultraviolet lamp (UVP 6 W and 365 nm wavelength), located at 58.5 cm high, to maintain a controlled light environment and avoid interference due to natural light. The images were taken by video capture. Videos of 10 minutes each were taken, with a capture rate of 120 frames per second (fps). Once the videos were obtained, they were separated into 72,000 images for each one, which were subjected to pre-processing.

Proposed model

The proposed model is shown in Figure 4. An image extracted from a video file is taken through pre-processing. The first step is to binary the image, using the Definition 11 with a threshold of 80, in this case depending on the shades of green. The image obtained is applied with the morphological aperture defined in 7, in order to eliminate noise generated by binarization. From the filtered image, called the current image, two processes are carried out: 1) the obtaining of the **Geometric Information** of interest, through Definition 11; this process determines the number of objects found, which correspond to the total number of centroids obtained in addition, the area of each object is calculated, to determine an average area, in experimentation, this value is 120 square pixels. If in the current image, the number of centroids matches the number of real objects and the area of each of them is equal to the average, it means that are no joined objects. The information is stored as a function of the coordinates of each centroid and **Distance Analysis** is carried out, which indicate the change of position of the centroids, is carried out, thus representing the movement of each object. However, this does not apply to all the images analyzed. Otherwise, it implies that they are not the total of real objects and a separation process must be carried out, since it is possible that there are objects attached to others, even with a minimum distance of one pixel. For this reason, the centroids and the average area of the objects are determined. These geometrical characteristics provide information on the number of objects detected in the image.

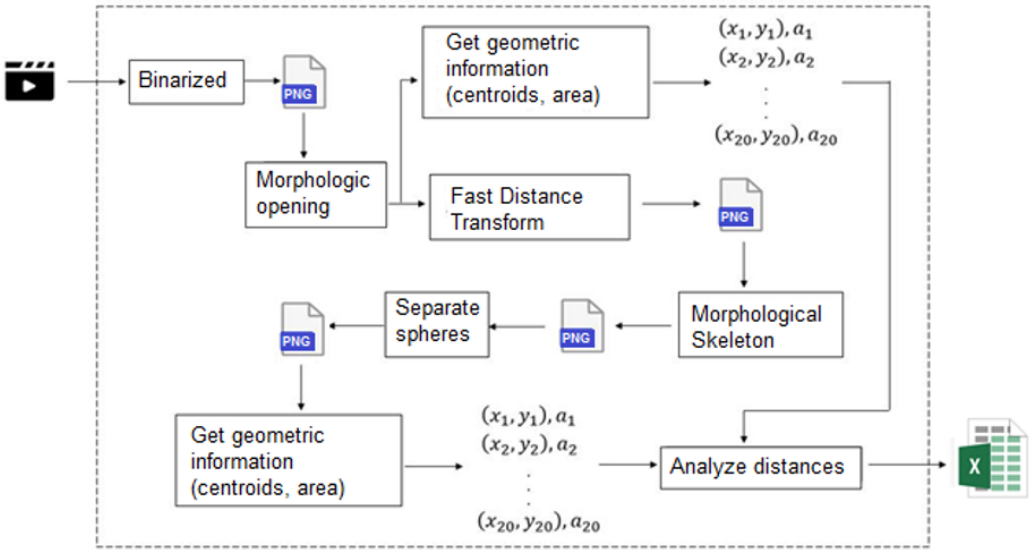

Fig. 4. Proposed segmentation model.

Therefore, if the area of an object is greater than the average area, in conjunction with the amount of centroids obtained, in principle it indicates the number of objects bound together, which implies that they must continue with the separation process. And 2) obtaining the FDT by Definition 4, with this it is possible to obtain the maps of distances of all the pixels of the objects, from the edge to the center, representing the shades less bright, to those of greater brightness, respectively and generates a new image to analyze, but now, depending on the shades of gray. The **Morphological Skeleton** process given by Definition 9 takes the image generated by the FDT process, obtains as skeleton pixels only the 3 distances generated by Definition 11, corresponding to the furthest points from the edge to the centre and in turn the brightest. The skeleton pixels that do not belong to these three maximum distances are removed from the skeleton, isolating the pixels that approach the center of each object that is stuck, in this part is where the separation or segmentation of the joined objects has been done, but leaving a set of skeleton pixels that define the original object and a new image is generated. The **Separate Spheres** process takes the resulting skeleton image and scans it until finding the set of pixels that defines each separate object. With that condition, the average of these sets of pixels is obtained by generating a single coordinate per object. These coordinates are the new centroids of the separated objects. Since the original radii of objects are approximately 11, the new centroids are taken as the basis for drawing circles of radius 6. Since with smaller radii, objects are prevented from re-joining once they have been segmented, this process creates a new image. Finally, the **Geometric Information** of the segmented image is obtained again, stored again and compared with the geometric information obtained after the morphological opening. The foregoing is in order to determine what geometrical information will be taken into account to perform the **Distance Analysis**, determine the change of position, the movement of the objects, and reincorporate the images to the video file. Create a file that stores said information of all objects and in this way, track each of them (Figure 4), which represent microalgae cells in the bioreactor Raceway.

3 Results and discussion

Tracer particles

There are different materials to use as tracer particles. In some works such as that of (Zeng *et al.*, 2016) aluminum oxide (Al_2O_3) particles with a diameter of 10 μm are used. The particles used in this work are 100 μm in size and are capable of fulfilling their

function. Particles up to 500 μm can be used, as long as their density is not greater than the density of the liquid, they float and are visible (Raffel *et al*., 2013). In addition, the proposed method is visual, so the size of the tracers does not need to be so small. The density of a microalgae culture in dilution is approximately equal to that of water (1,000 Kg/m^3), due to the low concentration of biomass (Sompech *et al*., 2012), however, the density of the microalgae cells is lower to the density of water. Therefore, the tracer particles were used as a dispersed phase, simulating the movement of microalgae. Thanks to the difference in density, the particles tend to float and behave as aggregates of cells in suspension, following different routes, caused by the currents of water flow.

Establishment of the bioreactor and system conditions

The systems described in the literature, referring to the capture of images in Raceway bioreactors, are limited to obtaining images by sections, a particular case is that of (Zeng *et al*., 2016), which makes use of particle image velocimetry (PIV). However, the conditions of your system are different from those proposed here. The present work describes the methodology to determine frames and videos of the complete bioreactor. In this way, you have a broader picture of the behaviour of the flow, without the need to make assumptions or adjustments of the trajectories described by the tracers. In Figure 5 a), the Raceway bioreactor under study can be seen, with white lighting and the position of the camera to obtain the videos.

Fig. 5. Imaging system, a) Front view of the system, showing the Raceway bioreactor with mechanical stirring and position of the camera for obtaining videos and images. b) Top view of the bioreactor, in which some tracer particles are observed.

Figure 5 b) is the representation of the top view of the system, where some particles with a green hue are appreciated. In this image, it is difficult to observe all of the microspheres, due to the fluorescence characteristic, although they are better visible when in contact with ultraviolet light. In general, in any system, tracer particles are difficult to see with the naked eye, either because of their size or because they require light. In particle tracking methods, the illumination source is usually pulsed laser lights (Kim *et al*., 2016).

Imaging and pre-processing

In biological systems, the main tool to determine the hydrodynamic behavior of Raceway bioreactors is computational simulation, which uses similar characteristics of microalgae, such as size, shape and density. Another option is the application of medium density particle image velocimetry (PIV). This consists of comparing images of tracer particles, determining velocity vectors and flow patterns (Sompech *et al*., 2012; Ali *et al*., 2014: Zeng *et al*., 2016). The present work is based on the PIV methodology, for particle tracking. As mentioned before, 72,000 images are obtained unlike other methodologies. A particular case is the one described (Kim *et al*., 2016) where only two frames of Raceway bioreactors are processed, and which also makes use of PIV. It should be noted that, the lower the number of frames analyzed, the error in the measurement increases, so minimum capture speeds of 30 fps are recommended, and if greater precision in the analysis is needed, 60 fps (Rodríguez and Roa, 2017).

The frames obtained from the pre-processed videos are shown in Figure 6, where a) represents the image in its original colors. In this part, it can be seen that the particles in contact with ultraviolet light, take on a green hue. However, they produce reflections of themselves in the water, there are also reflections in purple and violet tones, since the light causes an effect on the water. For this reason, the noise reduction was implemented in the images with the previously described thresholding algorithm, as well as the determination of the centroids, this is represented in Figure 6 b). It can be clearly seen how the shades of green, generated by the reflections of the particles, cause that in the thresholding, the objects that are very close, are seen as one. With this phenomenon, information loss occurs, since, instead of determining 20 centroids, the image shows 19. Figure 6c is the enlargement of a section containing four particles.

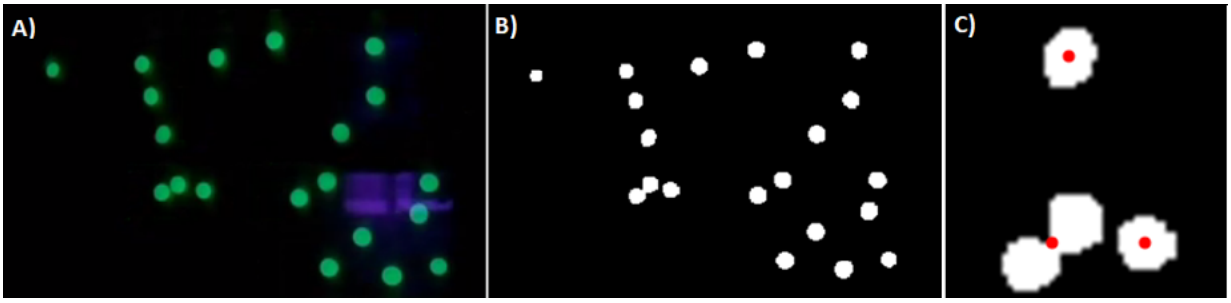

Fig. 6. a) Frame in original colors, all 20 tracers are green with some purple reflections due to light. b) Binarized frame and c) detection of centroids, with particle agglomeration.

However, with binarization the agglomeration of two objects becomes evident. Therefore, in the image processing, three individual objects are detected and information is lost when calculating the centroids.

Due to the proximity of the particles and to facilitate their detection, an algorithm was applied that allows the outline of each object to be drawn. From binary frames, the average area of individual particles was found to be 120 pixels. Dividing the area of the sets by the average area, you get an approximate amount of the number of particles found in the agglomeration. The number is compared and validated with the application of the segmentation algorithm. Although some authors suggest that thresholding and obtaining contours are methods for image segmentation (He *et al*., 2008), in this work it is taken as preprocessing and segmentation is considered in the application of the FDT.

3.1 Image processing and segmentation using the Fast Distance Transform

There are very complex techniques in image segmentation, which involve programming algorithms that include equations referring to differential and integral calculus (Pan *et al*., 2019; Liu *et al*., 2019). The number of frames processed in the proposed methodology is emphasized, which is 72,000, since in segmentation, few works analyse a large sequence of images. An example of this is that of (Rodríguez and Roa, 2017), in which sperm trajectories are constructed in a sequence of 30 frames. Rodríguez and Roa uses a segmentation stage by an adaptive method of Gaussian models and a prediction and correction mechanism, to follow up on the objects studied. On the other hand, it should be noted that the main characteristic of the FDT is its simplicity and practicality, because it is a linear algorithm and does not make excessive use of mathematics. The images under analysis, once pre-processed, were subjected to the Fast Distance Transform algorithm for their segmentation. Figure 7 a) shows the segmentation of the binarized frame. This segmentation detects the agglomeration of the particles and divides the image into sections of 100 x 100 pixels. The segment containing the set of two particles is highlighted, however in preprocessing it is detected as a single object. The individual centroid is obtained thanks to the application of the FDT (Figure 7 b), since it was possible to differentiate between the maximum value of the furthest pixel, from the contour of the object to its center of mass. The skeleton of each cluster of particles was drawn and thus the coordinates (x,y) of the pixels farthest from the contour were determined (Figure 7 c).

From the application of the FDT, the sections with joints were separated, as shown in Figure 7 d). Each particle is clearly differentiated and its centroid, in this case, are two objects that are reconstructed, in a size smaller than the average area (Figure 7 e). In this way, the FDT algorithm and the morphological skeleton make the necessary sweeps in the 72,000 frames of each video. Thus, the unions of particles contained in each image are divided, to determine the exact number of objects that make it up and to individually monitor each one of them. In particular, in this work tracers are monitored to determine flow patterns and speeds in a biological culture.

Figure 8 is a compilation of frames of the function of the set of algorithms under study of the Raceway system. Figures 8 a1) - 8 a3) show the progression of fluid movement in the Raceway bioreactor. The tracers are highlighted, shown in shades of green, in addition to the reflection of ultraviolet light in the water. The 20 particles and some agglomerations of them are clearly observed (Figures 8 a2) and 8 a3)). So there is a reduction of recognized particles, which will be processed for segmentation.

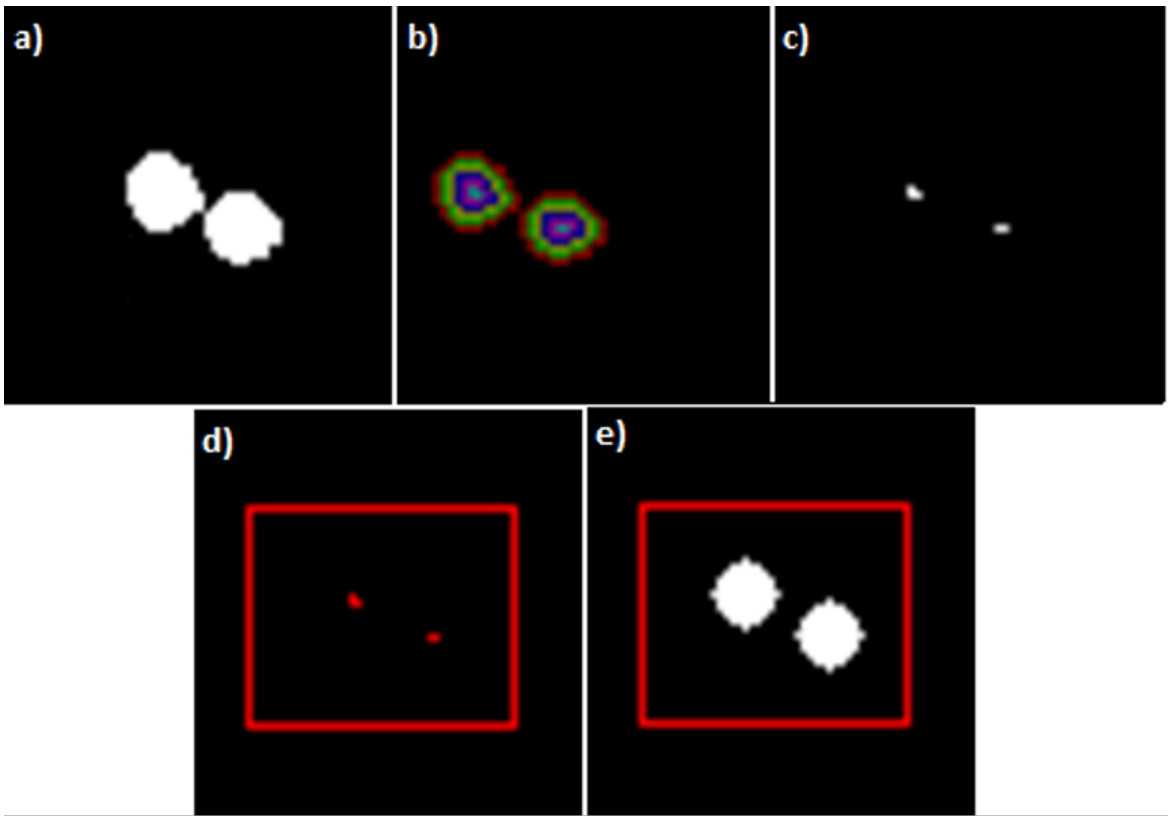

Fig. 7. Segmentation of agglomerated particles. a) Marking of agglomerate, b) The section highlights the FDT of two particles c) morphological skeleton of the particles. d) Delimitation of region and centroids of each particle. e) Reconstruction of the objects and individualization of the agglomerates, the particles are smaller due to the application of the FDT.

With the application of the algorithms, the contour of each particle was drawn, in different colors, to give individual follow-up to each object (Figure 8 b1). Figure 8 b2) shows the movement of the liquid, generated by a curved blade agitator, the flow currents drag the tracer particles, following the same trajectories of the water. After 10 minutes of agitation, the flow currents manage to distribute the particles throughout the system, generating a map of preferential routes that correspond to the flow patterns (Figure 8 b3).

A large part of the algorithms used in segmentation are focused on the analysis of a single image object. In general, they seek to have a uniform region (Vojodi *et al*., 2013; Yang *et al*., 2016), or a small sequence of frames, as already mentioned. In addition to this, there is a methodology that allows segmenting satellite images where the number and size of tree canopies are determined (Polak *et al*., 2009), but it has not been used for other applications. Compared to other image segmentation methodologies, the advantage of using FDT is its application to video processing. The results show that by coupling the FDT to high-speed video analysis, the processing error is decreased. Analysing a greater number of frames allows you to have more information, especially when it comes to calculating object paths. On the other hand, when the video capture speed is lower, the loss of information occurs, which is reflected in errors in the monitoring (Rodríguez and Roa, 2017). Furthermore, the segmentation obtained with this methodology (FDT) allows the separation of particles of various sizes and shapes. The main focus is the description of the movement of microalgae in Raceway bioreactors using spherical geometries. Microalgae present different cell morphologies, be they spherical, cylindrical, filamentous, etc., as well as organizations in sets of cells (Tomaselli, 2004).

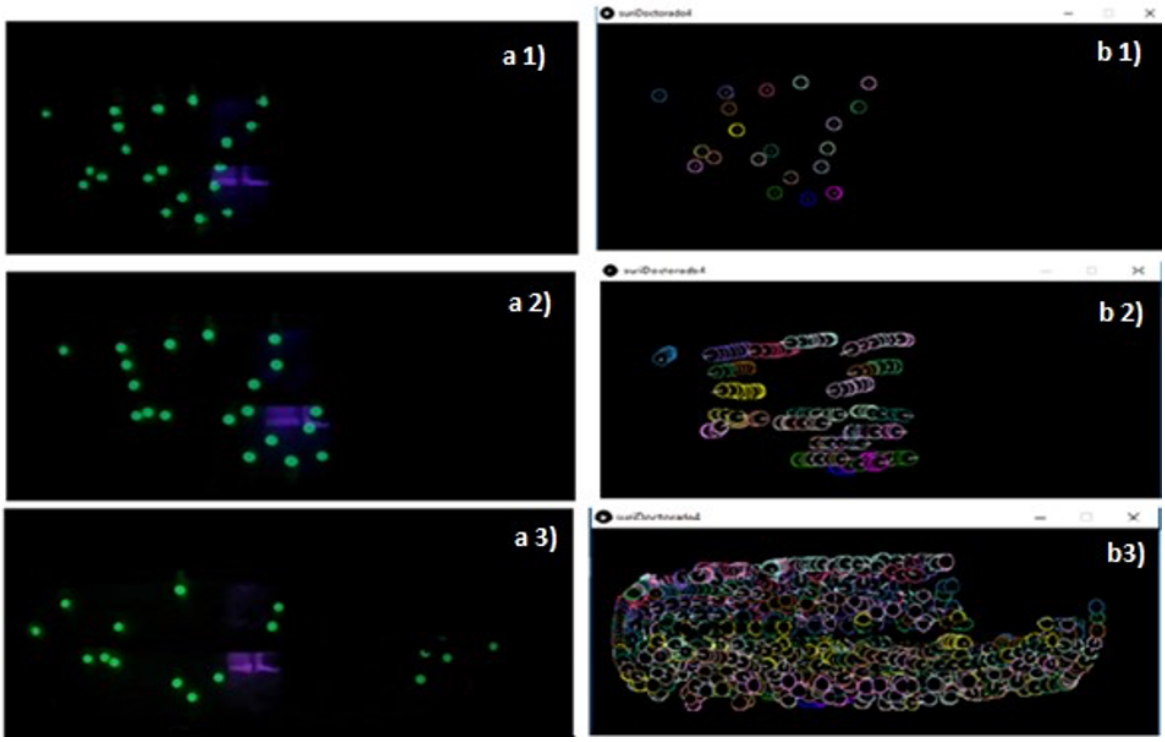

Fig. 8. Tracer particle path map, a) frames in original tones of the video, b) processed frames and mapping of the paths, according to the evolution of the video.

However, the algorithm is applicable to these morphologies, because it works with centroids. Additionally, the FDT allows to reconstruct any shape or geometry through the application of the morphological skeleton. The use of this methodology is useful in any field, where it highlights the importance of image segmentation and the analysis of individual objects.

Conclusions

In this work, a system for imaging and tracking particles in a Raceway bioreactor is proposed to describe the behavior of tracer particles, which simulate microalgae cells. It was suggested to apply a preprocessing of the frames before subjecting them to the segmentation algorithm. Similarly, the Fast Distance Transform (FDT) and the morphological skeleton were described and applied for the segmentation of images in a Raceway bioreactor. In addition, the reduction of the processing error was ensured, as well as the reduction of information loss in the tracking of the particles, due to the high capture speed (120 fps). With the algorithms used, a medium density particle image velocimetry method is proposed. With this method, the mapping of flow patterns in a biological culture system is obtained, although its application is not limited to this type of system. Perform image segmentation using FDT to apply in particle tracking method, can be an inexpensive and easy alternative to implement for hydrodynamic analysis in bioreactors of any type, not just for Raceways. This particle tracking method could be very used to determine scaling hydrodynamic parameters in bioreactors.

Acknowledgements

The first author received a scholarship from the Concejo Nacional de Ciencia y Tecnología (CONACYT), CVU 715281, for which he is grateful for the support provided by said institution, to study the Doctorado en Ciencias en Biotecnología within the postgraduate program of the Universidad Politécnica de Pachuca (UPP), included in the Padrón Nacional de Posgrados de Calidad (PNPC).

Nomenclature

A	Object area
(i, j)	Black pixel coordinate
M	Image height
N	Image width
x_c	Coordinate of the centroid on the x axis
y_c	Coordinate of the centroid on the y axis
(x, y)	White pixel coordinate

References

Akhlaghian Tab, F., Naghdy, G. and Mertis, A. (2005). Scalable multiresolution color image segmentation. *Signal Processing 86*, 1670-1687. https://doi.org/10.1016/j.sigpro.2005.09.016

Ali, H., Cheema, T. A., Yoon, H. S., Do, Y. and Park C. W. (2014). Numerical prediction of algae cell mixing. *Biotechnology and Bioengineering 112*, 297-307. http://doi.org/10.1002/bit.25443

Amaya-Zapata, S, Pulgarín-Velásquez, D. and Torres-Pardo, I. D. (2016). Desarrollo e implementación de un sistema de visión artificial basado en lenguajes de uso libre para un sistema seleccionador de productos de un Centro Integrado de Manufactura (CIM). *Lámpsako 15*, 43-50

Arcelli, C., Sanniti di Baja, G. and Serino, L.(2009). A parallel algorithm to skeletonize the distance transform of 3D objects. *Image and Vision Computing 27*, 666 -672. https://doi:10.1016/j.imavis.2008.07.014

Bai, X. D., Cao, Z. G., Wang, Y., Ye, M. N. and Zhu, L.(2014). Image segmentation using modified SLIC and Nyström based spectral clustering. *Optik 125*, 302-4307. https://doi.org/10.1016/j.ijleo.2014.03.035

Bautista-Monroy, S. S., Salgado- Ramírez, J. C., Téllez- Jurado, A., Ramírez.Vargas, M. R., Gómez-Aldapa, C. A., Pérez-Viveros, K. J., Medima-Moreno, S. A., Cadena-Ramírez, A. (2019). Hydrodynamic characterization in a Raceway bioreactor with diferent stirrers. *Revista Mexicana de Ingeniería Química 18*, 605-619. https://doi.org/10.24275/uam/izt/dcbi/revmexingquim/2019v18n2/Bautista

Borji, A. (2018). Negative results in computer vision: A perspective. *Image and Vision Computing 69*, 1-8. https://doi.org/10.1016/j.imavis.2017.10.001

Hanbury, A. and Marcotegui, B. (2008). Morphological segmentation on learned boundaries. *Image and Vision Computing 27*, 480-488. https://doi.org/10.1016/j.imavis.2008.06.012

He, L., Peng, Z., Everding, B., Wang, X., Han, C. Y., Weiss, K. L. and Wee, W. G. (2008). A comparative study of deformable contour methods on medical image segmentation. *Image and Vision Computing 26*, 141-163. http://doi.org/10.1016/j.imavis.2007.07.010

Hernandez-Aguirre, A., Casillas-Rodriguez, B.C., Cocotle-Ronzon, Y., Puebla, H., Hernandez-Martinez E. (2019). Monitoreo del tostado de café usando la Transformada de Fourier 2D de imagines. *Revista Mexicana de Ingeniería Química 18*, 231-240. https://doi.org/10.24275/uam/izt/dcbi/revmexingquim/2019v18n1/HernandezA

Kanhaiya, K., Sanjiv, M., Anupama S., Min, S. P. and Won Yang, J. (2015). Recent trends in the mass cultivation of algae in raceway ponds. *Renewable and Sustainable Energy Reviews 51*, 875-885. https://doi.org/10.1016/j.rser.2015.06.033

Kim, K. W., Lee, W. H., Lee, Y. H., Ali, H., Kwark, M. K. and Park, C. W. (2016). Particle Image Velocimetry measurement of hydrodynamic properties of Raceway pond with the effect of central wall. *Sensors and Materials 28*, 957-966. http://dx.doi.org/10.18494/SAM.2016.1257

La Serna Palomino, N. and Román Concha, U. (2009). Técnicas de segmentación en procesamiento digital de imágenes. *Revista de Ingeniería de Sistemas e Informática 6*, 9-16.

Liu, Y., He, C., Wu, Y. and Ren, Z. (2018). The L0-regularized discrete variational level set method for image segmentation. *Image and Vision Computing 75*, 32-43. https://doi.org/10.1016/j.imavis.2018.03.001

Liu, Y., He, C., Wu, Y. and Ren, Z. (2019). A binary level set variational model with L1 data term for image segmentation. *Signal Processing 155*, 193-201. http://doi.org/10.1016/j.sigpro.2018.08.017

Lizardi-Jiménez, M. A., and Gutiérrez-Rojas, M. (2011). Assessment of the local hydrodynamic zones in a three-phase airlift reactor: looking for the lowest liquid-phase Re. *Revista Mexicana de Ingeniería Química 10*, 59-65.

Loaiza Quintana, A. F., Manzano Herrera, D. A and Múnera Salazar, L. E. (2012). Sistema de visión artificial para conteo de objetos en movimiento. *El hombre y la máquina 40*, 87-101. http://www.redalyc.org/articulo.oa?id=47826850010

May-Cua, E.R., Toledano-Thompson, T., Alzate-Gaviria, L.M., Barahona-Pérez, L.F. (2019). A cylindrical-conical photobioreactor and a sludge drying bed as an efficient system for cultivation of the green microalgae *Coelastrum* sp. and dry biomass recovery. *Revista Mexicana de Ingeniería Química 18*, 1-11. https://doi.org/10.24275/uam/izt/dcbi/revmexingquim/2019v18n1/May

Pan, H., Liu, W., Li, L. and Zhou, G. (2019). A novel level set approach for image segmentation with landmark constraints. *Optik - International Journal for Light and Electron Optics 182*, 257-268, http://doi.org10.1016/j.ijleo.2019.01.009

Polak, M., Zhang, H. and Pi, M. (2009). An evaluation metric for image segmentation of multiple objects. *Image and Vision Computing 27*, 1223-1227. http://doi.org/10.1016/j.imavis.2008.09.008

Raffel, M., Willet, C. E. and Kompenhans, J. (2013). *Particle Image Velocimetry, a Practical Guide*, vol. 2, Springer, New York.

Rarrek, A., Mostertz, M., Kistenmacher, H., Rehfeldt, S., and Klein, H. (2016). Simulation and optimization of large open algae ponds. *Chemical Engineering Research and Design 114*, 220-235. http://dx.doi.org/10.1016/j.cherd.2016.08.018

Rodríguez-Mata, A. E., Flores-Colunga, G., Rangel-Peraza, J. G., Lizardi-Jiménez, M. A., and Amabilis-Sosa, L. A. (2019). Estimation of states in photosynthetic systems via chained observers: design for a tertiary wastewater treatment by using *Spirulina maxima* on photobioreactor. *Revista Mexicana de Ingeniería Química 18*, 273-287. https://doi.org/10.24275/uam/izt/dcbi/revmexingquim/2019v18n1/Rodriguez

Rodríguez-Montaña, D. F. and Roa-Guerrero, E. E. (2017). Detección de trayectorias de espermatozoides humanos mediante técnicas de procesamiento de video. *Revista Mexicana de Ingeniería Biomédica 38*, 115-125. http://dx.doi.org/10.17488/RMIB.38.1.8

Sabri, L. S., Sultan, A. J., and Al-Dahhan, M. H. (2018). Mapping of microalgae culturing via radioactive particle tracking. *Chemical Engineering Science 192*, 739-758. https://doi.org/10.1016/j.ces.2018.08.012

Salgado Ramírez, J. C. (2011). Memorias Asociativas en álgebra min y max robustas al ruido mezclado. Tesis de Doctorado en Ciencias de la Comunicación, Instituto Politécnico Nacional, México. https://www.repositoriodigital.ipn.mx/handle/123456789/7017

Solis-Méndez, A. Molina-Quintero, M., Oropeza-De la Rosa, E., Cantú-Lozano, D., Del Bianchi, V.L.(2020) study of agitation, color and stress light variables on *Spirulina platensis* culture in a vertical stirred reactor in standard medium. *Revista Mexicana de Ingeniería Química 19*, 481-490. https://doi.org/10.24275/rmiq/Bio616

Sompech, K, Chisti, Y. and Srinophakun, T. (2012). Design of raceway ponds for producing microalgae. *Biofuels 3*, 387-397. http://dx.doi.org/10.4155/bfs.12.39

Sotaquirá Gutiérrez, M. A., Plata Gómez, A. and Barrero Pérez, J. G. (2005). Uso de mapas de distancia en la segmentación de imágenes provenientes de geles de ADN. *Revista de la Facultad de Ingenierías Fisicomecánicas 4*, 25-33.

Tomaselli, L. (2004). The microalgal cell. In: *Handbook of Microalgal Culture: Biotechnology and Applied Phycology* (A.

Richnond Ed.), Pp. 3-19. Blackwell Science, Australia.

Vojodi, H., Fakhari, A. and Eftekhari Moghadam, A. M. (2013). A new evaluation measure for color image segmentation based on genetic programming approach. *Image and Vision Computing 31*, 877-886. http://doi.org/10.1016/j.imavis.2013.08.002

Yang, Y., Wang, Y. and Xue, X. (2016). A novel spectral clustering method with superpixels for image segmentation. *Optik 127*, 161-167. http://doi.org/10.1016/j.ijleo.2015.10.053

Yu, J., Huang, D. and Wei, Z. (2017). Unsupervised image segmentation via Stacked Denoising Auto-encoder and hierarchical patch indexing. *Signal Processing 143*, 346-353,. https://doi.org/10.1016/j.sigpro.2017.07.00

Zhang X., Li X., and Feng Y. (2015). A medical image segmentation algorithm based on bi-directional region growing. *Optik 126*, 2398-2404. https://doi.org/doi:10.1016/j.ijleo.2015.06.011

Zeng, F., Huang, J., Meng, C., Zhu, F., Chen, J. and Li, Y. (2016). Investigation on novel raceway pond with inclined paddle wheels through simulation and microalgae culture experiments. *Bioprocess Biosyst Eng 39*, 169-180. https://doi.org/10.1007/s00449-015-1501-9